J|A|C|S
COMMUNICATIONS

Published on Web 05/27/2006

Combined Hydrogen Production and Storage with Subsequent Carbon Crystallization

Angela D. Lueking,* Humberto R. Gutierrez, Dania A. Fonseca, Deepa L. Narayanan, Dirk Van Essendelft, Puja Jain, and Caroline E. B. Clifford

The Pennsylvania State University, 120 Hosler, University Park, Pennsylvania 16802-5000

Received January 20, 2006; E-mail: adl11@psu.edu

Development of a hydrogen economy will require significant advances in methods by which to produce, store, transport, and distribute hydrogen in an economically viable manner. Centralized hydrogen production methods currently in use are limited by an inefficient means to transport hydrogen to its point of use. Compressed and cryogenic storage methods do not meet density targets, and incremental advances in candidate solid-state storage materials are not likely to meet density or cost targets. Here we provide evidence of a combined hydrogen production and storage process that utilizes a low-cost carbon precursor that slowly evolves hydrogen at room temperature. The evolution of the trapped hydrogen appears to be kinetically limited as it continues in excess of one year; heating the material to modest temperatures accelerates hydrogen evolution. The parallel observation of a nanocrystalline diamond (NCD) byproduct suggests that the hydrogenative ball milling leads to a hydrogenated tetrahedral carbon form that rearranges to more stable crystalline carbon forms upon heating.

Reactive ball milling of Buck Mountain anthracite coal (BMT) with a cyclohexene hydrogen donor led to a carbon structure (referred to as BMT*) that decomposes upon heating to give molecular hydrogen. The term "hydrogen donor" is applied to cyclohexene as its dehydrogenation during milling leads to the following observations of molecular hydrogen evolution with thermogravimetric-mass spectroscopy (TG-MS) analysis. The TG-MS indicates the following qualitative hydrogen evolution ($m/z = 2$) for a sample analyzed at different times (Figure 1): an immediate increase in the hydrogen baseline (Type I),[1] followed by an increase at ~60 °C with a local maxima at ~150 °C (Type II), and a third increase at ~300 °C with a maxima at ~400 °C (Type III). Samples were exposed to air during sample transfer and during storage. The Type III hydrogen evolution was not accompanied by cyclohexene nor benzene (expected dehydrogenation product) evolution.[1] Types I and II hydrogen evolution at atmospheric pressure from the various BMT* samples ranges from 0.3 to 0.7 wt % depending on sample age (inset, Figure 1); however, these quantifications do not capture hydrogen evolution during storage and sample transfer. The Type I hydrogen evolution decreases with sample age (Figure 1).[1] Overall hydrogen evolution from the onset of sample heating to 750 °C is as much as 2.1 wt % after 3 days of storage under atmospheric conditions (inset, Figure 1). In comparison, hydrogen evolution from the BMT precursor ensues at 550 °C and is 0.4 wt % with no significant Type I baseline increase (Figure 1d).

In a parallel set of experiments, we heated BMT* to 1400 °C in argon, then attempted to remove metals by a series of acid and base treatments (BMT*-1400). Crystalline regions are observed at several locations in BMT*-1400, ranging in size from 5 to 35 nm. The crystalline regions are embedded in a graphitic carbon outer-layer (Figure 2b), and Fourier transform (FT) reveals a reciprocal-space lattice corresponding to the diamond crystal structure observed along the [011] zone axis and a lattice constant of 3.57 Å (Figure 2c,d). The 3.4 Å spacing of the shells surrounding the core is consistent with graphite, but discontinuities with periodicity of 2.0 Å (close to the (111) interplanar distance of diamond) suggest a sp^2-sp^3 hybridization transition. These diamond−graphite structures are similar to those reported previously after electron irradiation[2,3]

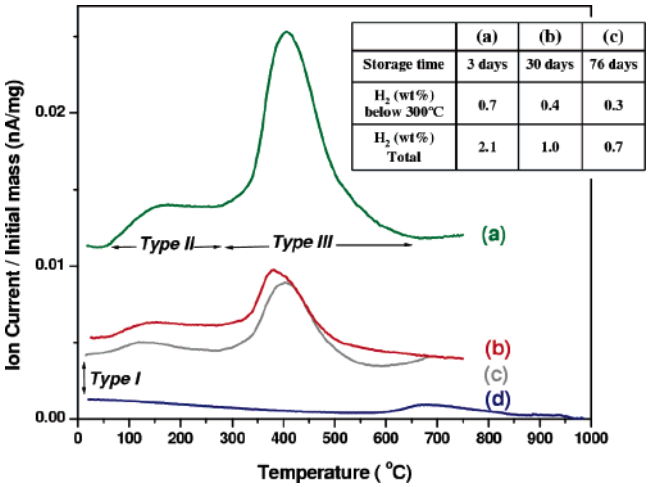

	(a)	(b)	(c)
Storage time	3 days	30 days	76 days
H_2 (wt%) below 300°C	0.7	0.4	0.3
H_2 (wt%) Total	2.1	1.0	0.7

Figure 1. TG-MS evolution ($m/z = 2$) for several preparations of BMT* (a−c) relative to the BMT coal precursor (d). The table (inset) summarizes the curve integration relative to a TiH_2 calibration. Type I indicates the observed immediate increase in the TG-MS signal (see text), not an arbitrary curve shift.

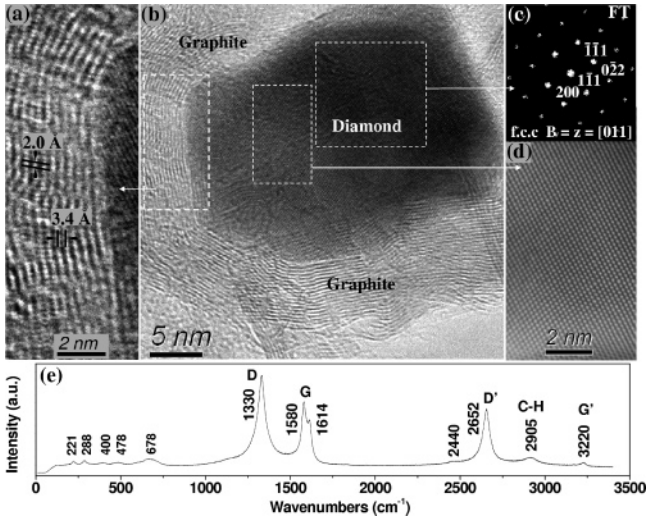

Figure 2. Representative HRTEM of observed crystalline regions (a−b). FT (c) and high-resolution (d) indicate a highly crystalline structure with a 3.56 Å lattice parameter. Visible Raman (633 nm) shows a split *G* peak (1580 and 1614), an increased *D′* peak (2652), and several low-frequency peaks (e).

10.1021/ja0604818 CCC: $33.50

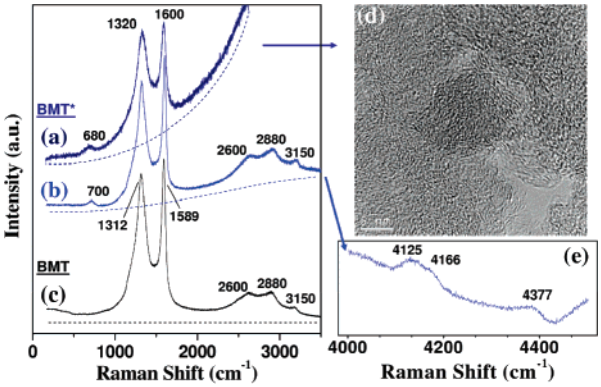

Figure 3. Visible Raman (633 nm) and BMT* samples after (a) 3 days and (b, e) 1 year, relative to (c) the BMT precursor. Dashed lines reflect observed background photoluminescence. (d) A representative HRTEM of the BMT* sample shows a defective (quasi-amorphous) carbon structure.

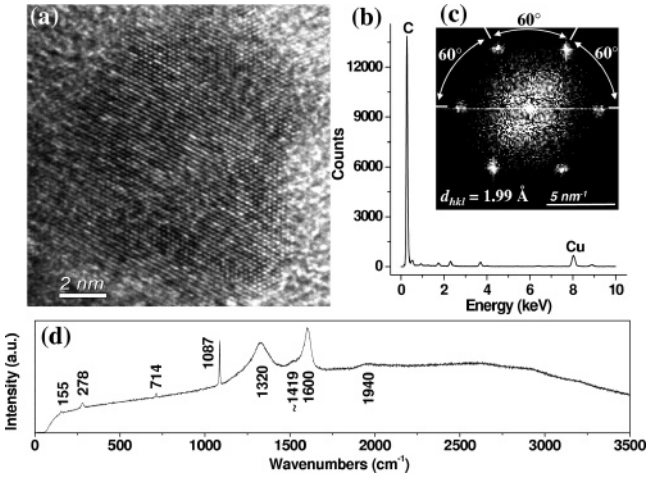

Figure 4. (a) HRTEM observation of crystalline carbon in BMT*^{P} surrounded by amorphous carbon. FT of this image (c) presents a six-fold symmetry, corresponding to crystalline planes with a 1.99 Å (d_{hkl}) spacing. EDX data (b) indicate the region is carbon based. Visible Raman spectra (d) of this sample indicate a broad *D* peak and several additional peaks relative to the BMT precursor.

and have been referred to as bucky diamond. Transition regions similar to Figure 2a are also observed that lack the inner core structure. Corresponding changes in the visible Raman spectra (633 nm, Figure 2e) may be attributed to structural doping (increased *D′* reflection at 2652 cm^{-1}) and localized sp^2 defects within sp^3-hybridized carbon, the so-called "dumbbell defect" (at 1620 cm^{-1}).[4,5] Low-frequency Raman modes arise that are consistent with either metal oxides or carbon: NCD has been reported to have a vibration at 496 cm^{-1},[6] and tetrahedral carbon has a low-energy tail at ~600 cm^{-1} in visible excitation.[7,8]

Rehybridization of sp^2 nanocarbons upon the introduction of hydrogen has been theoretically predicted. Hydrogen adsorption on planar graphite leads to distortion,[9] and doped nanocarbons will restructure and partially rehybridize to sp^3 carbon upon hydrogen exposure,[10] leading to an increased adsorption energy and stretching of the molecular hydrogen bond.[11] These effects may be more pronounced upon the application of high pressure[12] or resulting from hydrogen chemisorption.[13] These prior results are based on molecular simulations, and sp^3 rehybridization due to hydrogen exposure in carbon has not been previously observed experimentally, although hydrogen-induced crystallization has been reported for amorphous silicon.[14] These reasons led us to suspect that the parallel observations of hydrogen evolution and subsequent carbon crystallization may be related.

To further explore the role of hydrogen evolution in synthesis and crystallization, we further characterized BMT, BMT*, and BMT*^{P} (BMT*^{P} is BMT* treated with the same acid and base sequence used to purify BMT*-1400).[1] Diamondoids[10] and NCD[11] have been isolated from petroleum, but there have been no previous reports of their isolation from coal. We also find no analytical evidence for NCD in BMT or BMT*; quasi-amorphous carbon structures are typical for BMT* (see Figure 3d). BMT* has photoluminescence (Figure 3a) in visible (633 nm) Raman relative to the coal precursor (Figure 3c), which continues in excess of 1 year after preparation, with decreased intensity (Figure 3b). Photoluminescence has been empirically correlated to hydrogen content of tetrahedral amorphous carbons.[15] Unusual high-frequency Raman vibrations are observed for BMT*. In freshly prepared samples, the photoluminescence obscures these high-frequency peaks. One year after preparation, high-frequency peaks are no longer obscured by photoluminescence (Figure 3e, peaks at 4125, 4166, and 4377 cm^{-1}). The high-frequency peaks are near the Q-branch vibrations of molecular hydrogen (i.e., 4150−4160 cm^{-1}), which may be perturbed upon surface interaction, as demonstrated for in situ Raman hydrogen adsorption studies with carbon at cryogenic temperatures in a pressurized hydrogen atmosphere.[16−18] To the best of our knowledge, peaks in this range are not associated with carbon and the degree of photoluminescence is unusual; ongoing Raman investigations are underway with deuterated solvents to definitely assign the high-frequency peaks.

A crystalline carbon structure embedded in amorphous carbon was observed via HRTEM in BMT*^{P} (Figure 4a). The amorphous carbon-encapsulated structure converts to a bucky diamond structure with electron irradiation (data not shown), indicating the instability of this region. The crystalline structure of BMT*^{P} is different than that of BMT*-1400; the 6-fold symmetry of the FT from BMT*^{P} (Figure 4c) correlates with either a face centered cubic structure (zone axis [111]) or a close packed hexagonal structure (zone axis [0001]). The d_{hkl} spacing of 1.99 Å does not match graphite, diamond, or lonsdaleite. EDX analysis indicates this region is primarily carbon-based (Figure 4b). BMT*^{P} had a sharp Raman peak at ~1090 cm^{-1} and several low-frequency peaks (e.g., 155, 278, and 714 cm^{-1}), as shown in Figure 4d. The origin of these peaks is currently unknown and under investigation; the origin of peaks at ~1090 cm^{-1} are under debate in the diamond literature.

There are four potential driving forces for crystallization involved in the process: (i) a mechanical one during ball milling that may contribute to stress-induced crystallization or localized high-pressure regions upon impact; (ii) thermal restructuring of a less thermodynamically stable material, such as amorphous carbon; (iii) acid- or base-catalyzed carbon precipitation and/or restructuring; and (iv) the interaction between the hydrogen released from the hydrocarbon donor with the carbon bonds or terminal carbon edges in the coal. These four driving forces may act in combination to contribute to the complex structures. The relative contribution of each of these potential processes is currently under investigation.

The hydrogen evolution we see is somewhat comparable to previous ball milling reports, yet contains low-temperature hydrogen evolution (Types I and II) that we cannot solely attribute to cyclohexene dehydrogenation upon heating, as its intensity does not fully correlate with cyclohexene desorption.[1] Imamura et al. observed similar low-temperature hydrogen evolution, for magnesium milled with added graphite and organic solvents. Imamura attributed the low-temperature hydrogen evolution to magnesium hydride.[19] Our BMT coal contained inherent mineral matter,

including 0.06 wt % Mg, and transition metals introduced by the milling process (i.e., Fe, Ni, and Cr). The metals may catalyze structural transformation and cyclohexene dehydrogenation in the mill; however, the 1−2 wt % hydrogen evolution cannot be attributed solely to metals which make up only 5−10% of the sample. The high-frequency Raman vibrations and room temperature hydrogen evolution are atypical of metal hydrides and physical adsorption to carbon.

The Type III hydrogen evolution is quite similar to the work of Orimo et al.,[20] which included two hydrogen peaks at 650 and ∼1000 K. Combined with neutron diffraction, the hydrogen evolution was attributed to hydrogen intercalated between graphene layers and hydrogen bound to terminal carbon groups. Iron imparted to the sample during milling was later demonstrated to be a necessary condition for the observed hydrogen evolution.[21] Subsequent reports have varied the carbon precursor and found a gradual decrease in the onset temperature of hydrogen evolution, from ∼330 °C for graphite[22,23] to ∼300 °C for an activated carbon precursor,[21] and ∼230 °C for a SWNT.[23] The possibility of the formation of hydrogenated tetrahedral amorphous carbon was mentioned in the initial report of Orimo. The formation of a hydrogenated tetrahedral amorphous carbon is consistent with the data presented here, including hydrogen evolution, photoluminescence in Raman spectroscopy, high-frequency Raman vibrations, and the subsequent observation of sp^3-hybridized NCD regions. The hydrogen evolution from BMT anthracite coal milled with cyclohexene is significantly lower than that of graphite milled in high-pressure hydrogen. This may be due to the number of discontinuities and dangling bonds within the quasi-graphitic structure of BMT. The dangling bonds may be particularly reactive with cyclohexene in the high-energy mill, due to possible chemical reactions that lead to structural transformation, including free radical, Diels−Alder, and hydrogen abstraction reactions. Forthcoming studies support this statement: BMT* exhibits oxidation behavior characteristic of a "nongraphitizing" coal, whereas BMT is "graphitizing".[24] This behavior has been attributed to cross-links;[25,26] tight cross-linking within the coal structure may serve to "trap" molecular hydrogen and lead to the high-frequency Raman vibrations. Alternatively, the hydrogen may actually play a role in the formation of cross-linkages, similar to that demonstrated for hydrogen-induced crystallization of silicon, in which Si−H−Si bonds were demonstrated.[14]

A hydrogenated tetrahedral amorphous carbon with hydrogen evolution that is kinetically limited due to tight cross-linking may be an interesting option for distributed hydrogen production, particularly if the process can be optimized with low-cost carbon precursors and hydrogen donors. Hydrogen storage targets for solid-state materials have proven difficult to meet in the DOE target temperature and pressure range for materials that rely on reversible adsorption. Ongoing studies in our laboratory give initial indication that the hydrogen uptake may be reversible at moderate temperatures and pressures.[27] A distributed hydrogen production process that combines hydrogen production and storage process may offer improved *overall* system efficiency, as separately, both hydrogen production and hydrogen storage come at an energy penalty.

Acknowledgment. Dr. John Badding and Mr. Jacob Caulkins of the PSU Chemistry Department provided equipment time and assistance with Raman spectroscopy. Funding for the project has been provided by the Consortium for Premium Carbon Products from Coal (DEFC2603NT41874, Internal Agreement No. 2875-TPSU-DOE-1874), with partial support from PSU's Institutes for the Environment, Energy Institute, and Material Research Institute.

Supporting Information Available: Sample preparation, methods, TG-MS data, calibration, and baseline information. This material is available free of charge via the Internet at http://pubs.acs.org.

References

(1) See also Supporting Information.
(2) Kuznetsov, V. L.; Chuvilin, A. L.; Butenko, Y. V.; Malkov, I. Y.; Titov, V. M. *Chem. Phys. Lett.* **1994**, *222*, 343.
(3) Zaiser, M.; Banhart, F. *Phys. Rev. Lett.* **1997**, *79*, 3680.
(4) Orwa, J. O.; Nugent, K. W.; Jamieson, D. N.; Prawer, S. *Phys. Rev. B* **2000**, *62*, 5461.
(5) Prawer, S.; Nugent, K. W.; Jamieson, D. N.; Orwa, J. O.; Bursill, L. A.; Peng, J. L. *Chem. Phys. Lett.* **2000**, *332*, 93.
(6) Zhang, D. J.; Zhang, R. Q. *J. Phys. Chem. B* **2005**, *109*, 9006.
(7) Bacsa, W. S.; Lannin, J. S.; Pappas, D. L.; Cuomo, J. J. *Phys. Rev. B* **1993**, *47*, 10931.
(8) Ferrari, A. C.; Robertson, J. *Phys. Rev. B* **2001**, *64*, 075414.
(9) Ferro, Y.; Marinelli, F.; Allouche, A. *J. Chem. Phys.* **2002**, *116*, 8124.
(10) Froudakis, G. E. *J. Phys.: Condens. Mater.* **2002**, *14*, R453.
(11) Cheng, H.; Pez, G. P.; Cooper, A. C. *J. Am. Chem. Soc.* **2001**, *123*, 5845.
(12) Yildirim, T.; Gulseren, O.; Kilic, C.; Ciraci, S. *Phys. Rev. B* **2000**, *62*, 12648.
(13) Yildirim, T.; Gulseren, O.; Ciraci, S. *Phys. Rev. B* **2001**, *6407*, 075404.
(14) Sriraman, S.; Agarwal, S.; Aydil, E. S.; Maroudas, D. *Nature* **2002**, *418*, 62.
(15) Casiraghi, C.; Ferrari, A. C.; Robertson, J. *Phys. Rev. B* **2005**, *72*, 085401.
(16) Williams, K. A.; Eklund, P. C.; Kostov, M. K.; Cole, M. W. *Phys. Rev. Lett.* **2002**, *88*, 165502.
(17) Pradhan, B. K.; Sumanasekera, G. U.; Adu, K. W.; Romero, H. E.; Williams, K. A.; Eklund, P. C. *Physica B* **2002**, *323*, 115.
(18) Centrone, A.; Brambilla, L.; Zerbi, G. *Phys. Rev. B* **2005**, *71*, 245406.
(19) Imamura, H.; Kusuhara, M.; Minami, S.; Matsumoto, M.; Masanari, K.; Sakata, Y.; Itoh, K.; Fukunaga, T. *Acta Mater.* **2003**, *51*, 6407.
(20) Orimo, S.; Majer, G.; Fukunaga, T.; Zuttel, A.; Schlapbach, L.; Fujii, H. *Appl. Phys. Lett.* **1999**, *75*, 3093.
(21) Ichikawa, T.; Chen, D. M.; Isobe, S.; Gomibuchi, E.; Fujii, H. *Mater. Sci. Eng. B* **2004**, *108*, 138.
(22) Orimo, S.; Zuttel, A.; Schlapbach, L.; Majer, G.; Fukunaga, T.; Fujii, H. *J. Alloy Compd.* **2003**, *356*, 716.
(23) Hirscher, M.; Becher, M.; Haluska, M.; Quintel, A.; Skakalova, V.; Choi, Y. M.; Dettlaff-Weglikowska, U.; Roth, S.; Stepanek, I.; Bernier, P.; Leonhardt, A.; Fink, J. *J. Alloy Compd.* **2002**, *330*, 654.
(24) Burgess-Clifford, C. E.; Narayanan, D.; Van Essendelft, D. T.; Jain, P.; Lueking, A. D. Manuscript in preparation.
(25) Franklin, R. *Acta Crystallogr.* **1951**, *4*, 253.
(26) Franklin, R. *Proc. R. Soc. Ser. A* **1951**, *209*, 196.
(27) Narayanan, D.; Lueking, A. D. Manuscript in preparation.

JA0604818